Kinetic and Product Yield Study of the Heterogeneous Gas−Surface Reaction of Anthracene and Ozone

Nana-Owusua A. Kwamena,* Michael E. Earp, Cora J. Young, and Jonathan P. D. Abbatt

Department of Chemistry, University of Toronto, Ontario, Canada M5S 3H6

Received: October 25, 2005; In Final Form: January 13, 2006

Little quantitative information exists regarding the products of the heterogeneous reaction of polycyclic aromatic hydrocarbons (PAHs) and ozone. We have, therefore, performed the first quantitative study investigating the kinetics and products of the heterogeneous gas−surface reaction of anthracene and ozone as a function of ozone concentration and relative humidity (RH). The reaction exhibited pseudo-first-order kinetics for anthracene loss under dry conditions (RH < 1%) and the pseudo-first-order rate coefficients displayed a Langmuir−Hinshelwood dependence on the gas-phase ozone concentration, which yielded the following fitting parameters: the equilibrium constant for ozone adsorption, $K_{O_3} = (2.8 \pm 0.9) \times 10^{-15}$ cm^3 and the maximum pseudo-first-order rate coefficient, $k^I_{max} = (6.4 \pm 1.8) \times 10^{-3}$ s^{-1}. The kinetics were unchanged when experiments were performed at approximately 50% and 60% RH. In the product study, a nonlinear dependence, similar to a Langmuir adsorption plot, of the anthraquinone product yield as a function of ozone concentration was observed and resulted in the following fitting parameters: $K_{O_3} = (3.4 \pm 1.5) \times 10^{-15}$ cm^3 and the maximum anthraquinone yield, $ANQ_{max}\% = 30 \pm 18\%$. Experiments performed under higher relative humidity conditions (∼50% and 60% RH) revealed that the anthraquinone yield was unaffected by the presence of gas-phase water. It is noteworthy that both the anthracene loss kinetics and the anthraquinone yields have a similar dependence on the degree of ozone partitioning to the surface. This can be understood in terms of a mechanism whereby the rate-determining steps for anthracene loss and anthraquinone formation are both driven by the amounts of ozone adsorbed on the surface. Our results suggest that at atmospherically relevant ozone concentrations (100 ppb) the anthraquinone yield from the ozonolysis of anthracene under dry and high relative humidity conditions would be less than 1%.

1. Introduction

Polycyclic aromatic hydrocarbons (PAHs) are emitted into the atmosphere from combustion sources and many are known carcinogens.[1] Once emitted, semivolatile (3−4 rings) PAHs and those with lower volatility (more than 4 rings) may be found sorbed to particle surfaces. Pierce and Katz have shown that PAHs are primarily associated with particles <5 μm in size.[2] Particulate matter of this size can penetrate deep into the lungs, resulting in allergenic, mutagenic and carcinogenic responses.[1] Recent studies link increases in $PM_{2.5}$ to increases in hospital admissions.[3] In addition, long-term exposure to $PM_{2.5}$ has been associated with lung cancer and mortality from cardiopulmonary disease.[4,5] Reductions in aerosol-related health risks and improvements to urban air quality requires a better understanding of the chemical and physical mechanisms that control the fate and transport of atmospheric PAHs.

Past studies of atmospheric PAH degradation have focused on two areas: homogeneous gas-phase reactions and heterogeneous reactions with aerosol particles or proxies for aerosol surfaces. Homogeneous reactions with oxidants such as OH, O_3, and NO_x govern the fate of the gas-phase PAHs, whereas heterogeneous reactions between surface-bound PAHs and gas-phase atmospheric oxidants govern the fate of particle-bound PAHs. Heterogeneous reactions of surface-bound organics such as PAHs may change the microphysical properties of the particle by making it more hygroscopic and thereby enhancing its cloud nucleation properties.[6]

The kinetics of these transformations not only determines their environmental significance but also provides insight into the nature of the reaction mechanism. Benzo[*a*]pyrene (BaP), in particular, has been the focus of many past studies[7−11] investigating the transformations of surface-bound PAHs. The literature regarding the reactivity of BaP suggests some uncertainty in the results due to the different atmospheric oxidant concentrations, substrates and analytical methods used. Recent kinetic studies by Poschl et al.[8] and Kwamena et al.[12] have used the Langmuir−Hinshelwood reaction mechanism to describe the reaction between ozone and BaP adsorbed to soot and azelaic acid aerosols, respectively. A reaction occurring by this mechanism implies that one species (i.e., the PAH) is adsorbed to the particle surface and the second species (i.e., ozone) is initially in the gas phase. For the reaction to proceed, the gas-phase species must first adsorb onto the particle surface. Mmereki et al.[13,14] have also observed Langmuir−Hinshelwood behavior for the reaction of anthracene adsorbed to different coated aqueous surfaces and ozone.

Studies of the mechanism and the product yield of the heterogeneous reaction of anthracene and ozone have been largely ignored. The oxidation of PAHs is believed to result in the following oxidation products: quinones and ketones, as well as ring-opening products such as aldehydes and carboxylic acids.[15] Of the few studies that have been conducted investigating the ozonolysis of anthracene, anthraquinone has been identified as a product. For example, studies by Bailey et al.[16] involving ozone dissolved in different solvents identified products formed from the ozonolysis of anthracene that included

* Corresponding author. E-mail: nkwamena@chem.utoronto.ca.

10.1021/jp056125d CCC: $33.50
Published on Web 02/14/2006

anthraquinone and phthalic acid. Mmereki et al.[14] identified 9,10-anthraquinone as a product of the reaction of ozone with anthracene adsorbed at the air−aqueous interface and dry Teflon, but no product yield was obtained in their study.

Previous laboratory studies provide a framework for how the reaction between surface-adsorbed anthracene and ozone may proceed in the atmosphere, but a detailed reaction mechanism remains unknown. Therefore, in this study we focused on quantitatively investigating the product yield of 9,10-anthraquinone from the reaction of surface-bound anthracene and ozone. Particular attention was placed on 9,10-anthraquinone because it has been identified in atmospheric air and particulate matter samples.[17−19] Quinones and other oxidized PAHs (OPAHs) are either directly emitted into the atmosphere from combustion sources [20,21] or formed as products from the photooxidation of PAHs.[22−25] Similar to PAHs, OPAHs are receiving increased research attention because the moderately polar fraction of environmental samples, which includes OPAHs such as quinones, have been shown to have direct-acting mutagenicity[17,26] and may even be more mutagenic that the parent PAH.[22]

Because OPAHs are more oxidized and less volatile than the parent PAHs, they are generally found sorbed to particles. Depending on their lifetimes, OPAHs may react with atmospheric oxidants; however, estimating their reaction lifetimes has been difficult because of the observed differences in the reactivity of OPAHs in laboratory studies.[27] A better understanding of the mechanism for quinone formation and its fate in the atmosphere is integral in determining the effects of quinones on human health.

In the following, we report kinetic experiments on the reaction between anthracene coated on Pyrex tubes—a proxy for an atmospheric aerosol surface inert to oxidation—and gas-phase ozone. In particular, the kinetics and product yields were studied as a function of both ozone concentration and relative humidity to determine if the Langmuir−Hinshelwood mechanism previously observed for the oxidation of surface-bound BaP also applies to this reaction system and if the product yields are similarly affected. We believe that this is the first study to quantify a product of this gas−surface reaction.

2. Experimental Section

2.1. Exposure Cell and Sample Preparation. An experimental procedure was developed to investigate the heterogeneous gas−surface reaction of anthracene with ozone from two perspectives: a kinetic and a product study (Figure 1). The effects of ozone concentration and relative humidity (RH) on the kinetics and product yield were determined. Pyrex tubes (l = 9.0 cm, d = 1.8 cm, SA = 50.9 cm^2) were used as the proxy for an inert aerosol. Prior to use, the tubes were rinsed with extracting solvent (5% dichloromethane/ 95% acetonitrile), cleaned with soap and water and air-dried. The inner surface of the Pyrex tubes was coated with 1 mL of a 1 ppm solution of anthracene in acetonitrile. The solvent was allowed to evaporate, leaving an anthracene surface coverage of 6.7×10^{13} molecules cm^{-2}, assuming uniform dispersal. The tubes were placed in a horizontally oriented flow tube where the anthracene was exposed to either a mixture of N_2/O_2 or $N_2/O_2/O_3$ for control or product/kinetic study experiments, respectively. The total flow through the system was between 220 and 340 sccm. For the experiments performed at higher relative humidities a portion of the N_2 flow was passed through a water bubbler before entering the flow tube. A hygrometer (VWR International) was used to determine the RH of the total flow. The flow tube was operated at ambient temperature and pressure conditions (293 K, 1 atm).

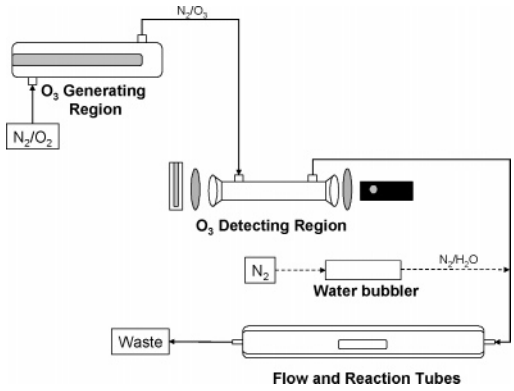

Figure 1. Experimental setup for the product and kinetic studies of surface-bound anthracene and ozone. Pyrex tubes coated with anthracene were exposed to ozone in a horizontally oriented flow tube. Ozone was generated by passing a mixed flow of O_2 and N_2 over a mercury pen-ray lamp and detected by using a second mercury pen-ray lamp. Different ozone concentrations were achieved by varying the ratio of O_2 and N_2 passing over the mercury pen-ray lamp. Following ozone exposure, the samples were extracted and analyzed using HPLC with ultraviolet detection. For the experiments performed at higher relative humidities, a portion of the flow was sent through a water bubbler before entering the flow tube. A hygrometer was used to measure the RH of the total flow entering the flow tube.

2.2. Ozone Generation and Detection. Ozone was generated by ultraviolet irradiation of a mixed flow of O_2 and N_2 by a mercury pen-ray lamp (length 23 cm, UVP Inc.) in a homemade Pyrex chamber and detected by absorption at 254 nm using a second mercury pen-ray lamp (length 5.4 cm, UVP Inc.) placed in front of a 10.3 or 50 cm absorbance cell with quartz windows at either end. The ozone concentration was controlled by varying the ratio of O_2 to N_2 passing over the pen-ray lamp. An interference filter (Esco Products) that passed 254 nm radiation was placed in front of an ultraviolet sensitive photodiode (Boston Electronics Corp.) at the other end of the absorbance cell to determine the ozone concentration entering the flow tube. The flow tube ozone concentrations investigated under dry conditions were $(0-9.1) \times 10^{15}$ molecules cm^{-3}. The high relative humidity experiments performed for the kinetic and product studies were conducted with ozone concentrations of 8.2×10^{13} and 1.5×10^{15} molecules cm^{-3} at 48% and 57% RH, respectively. The exposure time between the anthracene coated on the Pyrex tubes and ozone ranged from 2 to 60 min. For each exposure time a different Pyrex tube coated with anthracene was exposed to ozone. At least four replicate samples were obtained for each exposure time at a given ozone concentration.

2.3. Analytical Detection. Following ozone exposure, the tubes were extracted twice using 1 mL rinses of 5% dichloromethane/95% acetonitrile containing 2 ppm benz[*a*]anthracene-7,12-dione, which was used as the internal standard. A HPLC system from Perkin-Elmer (Series 200 LC pump) was interfaced to an ultraviolet detector (Perkin-Elmer, LC-240). The system was equipped with a C_{18} guard column (Adsorbosil, 7.5 mm × 4.6 mm × 5 μm, Alltech) coupled to a C_{18} reversed-phase chromatographic column (Supelcosil, 220 mm × 4.6 mm × 5 μm, Supelco). Analysis was performed using a 20 μL injection volume and an isocratic elution of acetonitrile−water (75:25 v/v, HPLC grade Fischer Scientific and 18 MΩ water, respectively) at a constant flow rate of 1 mL min^{-1}. A detection wavelength of 251 nm was used to monitor the anthracene, anthraquinone and benz[*a*]anthracene-7,12-dione signals. The Turbochrom software package (Perkin-Elmer) was used to integrate the chromatographic peaks. Identification of the peaks was achieved by comparing retention times to authentic

standards. The degradation of anthracene and the appearance of anthraquinone were quantified using benz[*a*]anthracene-7,12-dione as an internal standard over a concentration range of a few ppb to a few ppm.

2.4. Sample Extraction Efficiency. Particular attention was focused on ensuring that the extraction efficiencies for the reactants and the products of this reaction were well characterized. A series of spike and recovery experiments were performed in this regard. Initial studies focused on finding the best solvent(s) for extracting anthracene and anthraquinone. Subsequent control experiments were conducted to identify the potential interference of secondary reactions on the observed results.

Pyrex tubes were spiked with anthracene and anthraquinone to yield a surface concentration of 6.7×10^{13} molecules cm^{-2} and extracted using the following solvents individually: acetonitrile, dichloromethane, ethyl acetate and hexane. Acetonitrile was found to have the highest extraction efficiency of the four solvents tested. The use of dichloromethane and ethyl acetate as the extraction solvents resulted in poor chromatography that could not lead to quantification of the peaks. Different amounts of dichloromethane were added to acetonitrile, ranging from 5% to 10%, to increase the polarity of the acetonitrile extraction solvent. The most suitable extraction solvent for this study was determined to be 5% dichloromethane/95% acetonitrile. To improve the consistency of the extraction method, it was also important that the extraction solvent coat the entire surface of the Pyrex tube. Spike and recovery experiments for anthracene and anthraquinone revealed efficiencies of $57 \pm 3\%$ and $90.0 \pm 0.3\%$, respectively. The peak intensities were normalized before further analysis.

The following control experiments were performed to ensure that the observations being made were due to the reaction between anthracene and ozone and not due to other side reactions in the flow tube or during the extraction process:

1. Pyrex tubes were coated with anthracene and anthraquinone, individually, and exposed to N_2/O_2 for 20−30 min. Recoveries for anthracene and anthraquinone were consistent with the extraction efficiencies noted above. From this experiment it was concluded that blowoff from the surface to the gas phase was not a significant source of analyte loss.

2. Anthraquinone was coated on Pyrex tubes and exposed to ozone at the highest ozone concentration (9.1×10^{15} molecules cm^{-3}) investigated for 30 min. A recovery of $101 \pm 0.3\%$ after accounting for extraction efficiency indicated that ozone was not reacting with anthraquinone.

3. Last, to ensure that the intermediates from the reaction of anthracene and ozone were not reacting with anthraquinone to cause a reduction in our anthraquinone yields, tubes were spiked with anthracene and anthraquinone and exposed to the highest ozone concentration (9.1×10^{15} molecules cm^{-3}) investigated for 40 min. The anthraquinone yield determined from this control experiment was the same as the expected anthraquinone yield at high ozone concentrations indicating no such reaction was occurring.

To summarize, a solution of 5% dichloromethane/95% acetonitrile was found to be the most suitable extraction solvent for this study, resulting in extraction efficiencies of $57 \pm 3\%$ and $90.0 \pm 0.3\%$ for anthracene and anthraquinone, respectively. The uncertainties were determined at the 95% confidence interval. Control experiments revealed that blowoff, anthraquinone loss due to reaction with ozone and the interaction between reaction intermediates and anthraquinone in the presence of ozone did not contribute to the observed decays and product formations.

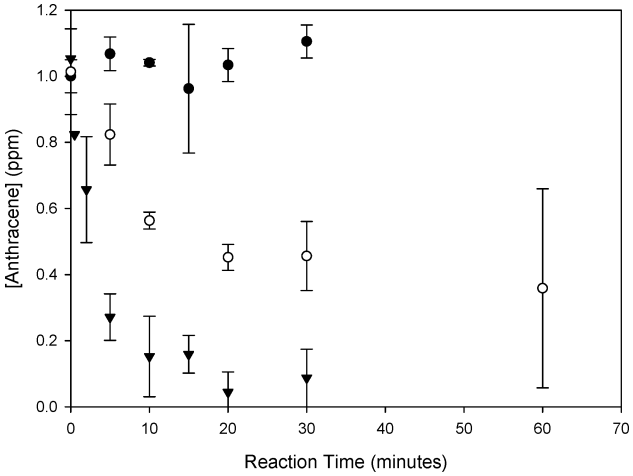

Figure 2. Anthracene concentration as a function of ozone exposure time in the flow tube. The initial anthracene surface coverage was 6.7×10^{13} molecules cm^{-2}. This figure presents the raw data at the two ozone concentration limits. Symbols indicate ozone mixing ratios: black circles, no ozone; open circles, 1.5×10^{14} molecules cm^{-3} of ozone; black inverted triangles, 9.1×10^{15} molecules cm^{-3} of ozone.

2.5. Chemicals. All chemicals were reagent grade and used without further purification. Anthracene (99%), anthraquinone (>97%) and benz[*a*]anthracene-7,12 dione (>98%) were purchased from Sigma-Aldrich. HPLC grade dichloromethane and acetonitrile were obtained from Sigma-Aldrich and Fisher Scientific, respectively. Ultrahigh purity N_2 and O_2 were obtained from BOC Gases Canada.

3. Results

3.1. Kinetics of Surface-Bound Anthracene and Ozone. The kinetics of the heterogeneous reaction between anthracene adsorbed on Pyrex tubes and gas-phase ozone were investigated as a function of gas-phase ozone concentration and relative humidity (RH). The kinetics were determined by monitoring anthracene loss as a function of ozone exposure time as illustrated in Figure 2, where data are presented at the two ozone concentration limits (1.5×10^{14} and 9.1×10^{15} molecules cm^{-3}). It is apparent that not all of the anthracene reacts away even at high ozone concentrations and long exposure times. We hypothesize that some of the anthracene is buried and therefore unavailable to react with ozone having been deposited as clumps or islands as opposed to being uniformly dispersed.

A monolayer of anthracene corresponds to approximately 1×10^{14} molecules cm^{-2} on the basis of its molecular cross section of 1 nm^2.[28] For typical experiments and assuming uniform coverage, the anthracene surface coverage was approximately 6.7×10^{13} molecules cm^{-2}, which corresponds to 0.7 monolayers. To test if the anthracene was being deposited as clumps or being uniformly dispersed, we coated the Pyrex tubes with an anthracene surface coverage of 3.4×10^{13} molecules cm^{-2} (0.3 monolayers) and 3.4×10^{14} molecules cm^{-2} (3 monolayers), which corresponds to half and five times the amount of anthracene used throughout the rest of this study. In the experiments performed with five times the anthracene surface coverage, one would assume that a significant portion of the anthracene was buried and unavailable to react with ozone. Our results revealed that at this high anthracene surface coverage, a larger fraction (75%) of the anthracene remained unreacted after long exposures to high ozone concentrations.

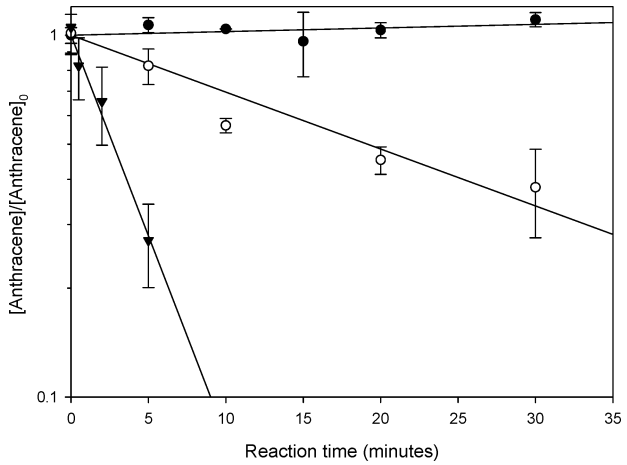

Figure 3. Kinetics of surface-bound anthracene and ozone under dry conditions. These are the same data as in Figure 2 corrected for the buried amount. The pseudo-first-order rate coefficient was determined from the slope of the uncertainty-weighted linear least-squares fit at each ozone concentration. Symbols indicate ozone mixing ratios: black circles, no ozone; open circles, 1.5×10^{14} molecules cm^{-3} of ozone; black inverted triangles, 9.1×10^{15} molecules cm^{-3} of ozone.

By reducing the surface coverage to half of what was used throughout this study, we still observed 25% unreacted anthracene after ozone exposure. With a low anthracene surface coverage (3.4×10^{13} molecules cm^{-2}) on the Pyrex tubes, we assumed that it was more likely that the anthracene was present as a smooth, uniform layer and therefore there would be no unreacted anthracene after ozone exposure. However, our observations of unreacted anthracene at both high and low anthracene surface coverages suggests that the anthracene was not being deposited as a smooth, uniform layer but more likely as clumps or islands under all conditions. In this form only a fraction of the anthracene is at the surface and available to react with ozone whereas some anthracene remains buried underneath.

The kinetics were determined by using the initial decay regions of the plots in Figure 2, as shown in Figure 3. To address the issue of burial for our kinetic analysis, the unreactive, buried fraction was subtracted from each point. For example, for the low ozone case (1.5×10^{14} molecules cm^{-3} in Figure 2), we subtracted the value at 60 min as our background value. The reaction is reasonably described by first-order kinetics given the linearity of the kinetic plots (Figure 3). The plots were fit with an uncertainty weighted-least-squares fit, and therefore, the shorter times dominate because they have the least uncertainty. The pseudo-first-order rate coefficient ($k^{\mathrm{I}}_{\mathrm{obs}}$) was obtained from the slopes of the uncertainty-weighted linear least-squares fit of the kinetic plots at each ozone concentration studied and its standard error was determined as the uncertainty of the slope at the 95% confidence interval.

The pseudo-first-order rate coefficients as a function of gas-phase ozone concentration are summarized in Figure 4. The shape of Figure 4 is consistent with a Langmuir−Hinshelwood reaction mechanism. This mechanism was first suggested by Poschl et al.[8] for PAH oxidation by ozone in their investigation of the reaction of surface-bound BaP on soot aerosols and ozone. According to this mechanism, one species is present on the surface and a second species is in equilibrium between the gas phase and the particle surface. A reaction can only proceed once the gas-phase species has adsorbed onto the surface; however, there are a limited number of sites to which it can adsorb. Therefore, at some gas-phase ozone concentration saturation of the surface occurs. Once saturation occurs, the rate of the reaction becomes saturated as well and thus becomes independent of the ozone concentration. This behavior is demonstrated in Figure 4 as the $k^{\mathrm{I}}_{\mathrm{obs}}$ begins to plateau at ozone concentrations greater than 1×10^{15} molecules cm^{-3}.

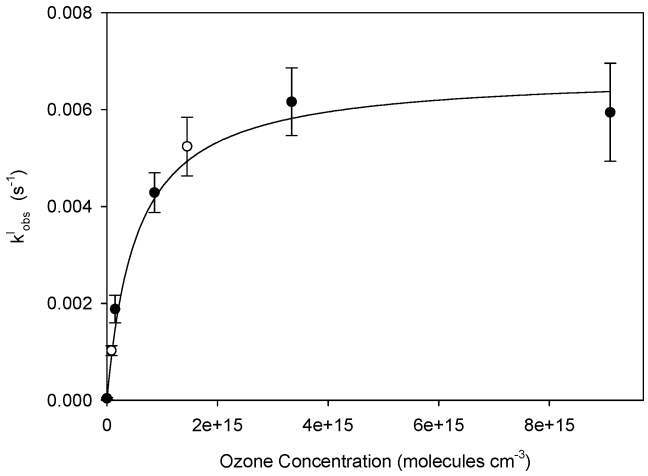

Figure 4. Pseudo-first-order rate coefficients ($k^{\mathrm{I}}_{\mathrm{obs}}$) as a function of gas-phase ozone concentration under dry and high relative humidity conditions. The plot summarizing the kinetics under dry conditions (black circles) was fitted using a nonlinear least-squares fit of eq 2 using the Levenberg−Marquardt algorithm in the Origin 6.0 data analysis software package. The standard error was obtained from the statistical error of the nonlinear least-squares fit at the 95% confidence interval. The fitting parameters for the kinetics under dry conditions, $K_{\mathrm{O_3}}$ and $k^{\mathrm{I}}_{\mathrm{max}}$, are listed in Table 1. The symbols indicate the relative humidity conditions: black circles, dry (<1% RH); open circles, elevated relative humidity (8.2×10^{13} and 1.5×10^{15} molecules cm^{-3} at 48% and 57% RH, respectively).

The parameters that describe the Langmuir−Hinshelwood reaction mechanism can be obtained by modeling the relationship between $k^{\mathrm{I}}_{\mathrm{obs}}$ and the gas-phase ozone concentration ([O_3(g)]) using the following equation, which is a modified version of the Langmuir equation:

$$k^{\mathrm{I}}_{\mathrm{obs}} = \frac{k^{\mathrm{II}}[\mathrm{SS}]K_{\mathrm{O_3}}[\mathrm{O_3(g)}]}{1 + K_{\mathrm{O_3}}[\mathrm{O_3(g)}]} \quad (1)$$

where k^{II} is the second-order surface rate coefficient, [SS] is the number of surface sites and $K_{\mathrm{O_3}}$ is the ozone gas-to-surface equilibrium constant. Equation 1 can be modified to yield

$$k_{\mathrm{obs}}{}^{\mathrm{I}} = \frac{k_{\mathrm{max}}{}^{\mathrm{I}}K_{\mathrm{O_3}}[\mathrm{O_3(g)}]}{1 + K_{\mathrm{O_3}}[\mathrm{O_3(g)}]} \quad (2)$$

where $k^{\mathrm{I}}_{\mathrm{max}}$ is the maximum rate coefficient that would be observed at high ozone concentrations. From eqs 1 and 2, it can be seen that $k^{\mathrm{I}}_{\mathrm{max}}$ is a product of the second-order surface rate coefficient and the number of surface sites for the gas-phase reactant (i.e., ozone). The plot in Figure 4 was fitted using a nonlinear least-squares fit of eq 2. The statistical error of the nonlinear least-squares fit was used to calculate the standard error at the 95% confidence interval. The fitting parameters yielded $K_{\mathrm{O_3}}$ and $k^{\mathrm{I}}_{\mathrm{max}}$ as listed in Table 1.

The effect of relative humidity on the kinetics was determined by performing high RH experiments at high and low ozone concentrations. The experiments were performed at ozone concentrations of 8.2×10^{13} and 1.5×10^{15} molecules cm^{-3} at 48% and 57% RH, respectively. As in the dry case, the linearity of the kinetic plots was consistent with first-order kinetics. The pseudo-first order rate coefficients obtained under higher relative humidity conditions are statistically indistinguishable from the

TABLE 1: Fitting Parameters for Figures 4 and 5[a]

	substrate	$10^{15}K_{O_3}$ (cm^3)	$10^3 k^I_{max}$ (s^{-1})	ANQ yield (%)
this work (Figure 4[b])	Pyrex glass and anthracene	2.8 ± 0.9	6.4 ± 1.8	
this work (Figure 5[c])	Pyrex glass and anthracene	3.4 ± 1.5		30 ± 18

[a] The uncertainties are reported at the 95% confidence level. [b] Figure 4 was fitted using eq 2. [c] Figure 5 was fitted using eqs 3 and 4.

pseudo-first-order rate coefficients obtained under dry conditions. This is shown by the agreement of rate coefficients obtained at high relative humidities with the Langmuir−Hinshelwood kinetic plot for kinetics under dry conditions (see Figure 4).

3.2. Product Identification and Yields. The product yield of 9,10-anthraquinone from the heterogeneous reaction of surface-bound anthracene and ozone was studied as a function of ozone concentration and relative humidity. The gas-phase ozone concentration range in the flow tube under dry conditions was $(0-9.1) \times 10^{15}$ molecules cm^{-3}. Upon exposure of the anthracene to ozone, a decrease in the anthracene signal was observed with an accompanying growth of a peak that was identified as 9,10-anthraquinone on the basis of retention time comparison to commercially available standards. We also saw evidence of phthalic acid formation in our samples; however, we were unable to obtain quantitative product yields due to difficulties with chromatography. Therefore, we focused on quantifying the amount of anthraquinone that was produced by the ozonolysis of anthracene. The concentrations of anthracene and anthraquinone were determined at each exposure time by interpolation of an internal standard calibration curve using benz[*a*]anthracene-7,12-dione as the internal standard. The anthraquinone yields were calculated when it was determined that the reaction was complete (i.e., the plateau region of Figure 2). The yields were calculated by dividing the amount of anthraquinone formed by the amount of anthracene that had reacted.

A plot of the anthraquinone product yield as a function of gas-phase ozone concentration shows a nonlinear dependence (Figure 5). Initially, there is a linear increase in the anthraquinone product yield, but starting at an ozone concentration of 1×10^{15} molecules cm^{-3}, the anthraquinone product yield begins to level off to a maximum yield of approximately 30%. The dependence of the product yield on the gas-phase ozone concentration indicates that the rate-limiting step for anthraquinone formation is dependent on the concentration of ozone on the surface. Given the similarity of the shape of the plot of the anthraquinone product yield as a function of ozone concentration to the kinetics plot in Figure 4, we fit Figure 5 using the following equation:

$$\text{ANQ } \% = \frac{a[O_3(g)]}{1 + b[O_3(g)]} \tag{3}$$

where *a* and *b* are fitting parameters. To determine the meaning behind these fitting parameters, we reexamine Figure 4 and its fit to eq 2. The value for fitting parameter *b* is, within experimental error, in agreement with the K_{O_3} obtained for the kinetic study described in Figure 4 (see Table 1). We, therefore, suggest that the *b* parameter is analogous to the equilibrium constant for ozone adsorption (K_{O_3}). Further, the k^I_{max} describes the maximum pseudo-first order rate that would be observed at high ozone concentrations, which graphically translates to the asymptote for the plot depicted in Figure 4. Examining Figure 5 at high ozone concentrations shows the maximum anthraquinone product yield approaches an asymptote of approximately 30%. Therefore, if we assume eq 3 takes the same form as eq 2, the *a* parameter is equal to the product of the maximum anthraquinone product yield observed at high ozone concentrations (ANQ_{max} %) and the K_{O_3}. As a result, eq 3 can be rewritten as

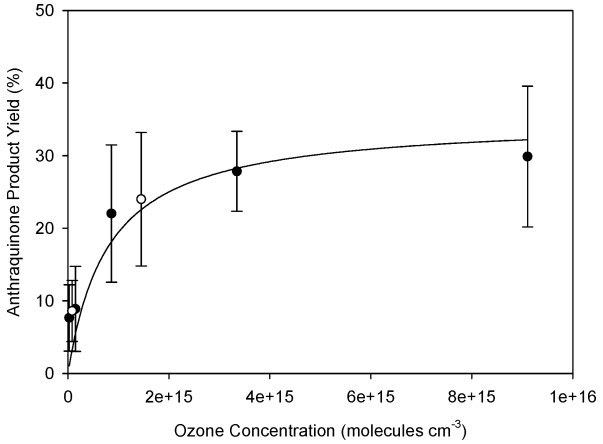

Figure 5. Anthracene product yields as a function of gas-phase ozone concentration under dry and high relative humidity conditions. The plot summarizing the product yields under dry conditions was fitted using a nonlinear least-squares fit of eq 3 using the Levenberg−Marquardt algorithm in the Origin 6.0 data analysis software package. The standard error was obtained from the statistical error of the nonlinear least-squares fit at the 95% confidence interval. The fitting parameters for the product yield under dry conditions, K_{O_3} and ANQ_{max} %, are listed in Table 1. The symbols indicate the relative humidity conditions: black circles, dry (<1% RH); open circles, elevated relative humidity (8.2×10^{13} and 1.5×10^{15} molecules cm^{-3} at 48% and 57% RH, respectively).

$$\text{ANQ } \% = \frac{\text{ANQ}_{max}\,\%\, K_{O_3}[O_3(g)]}{1 + K_{O_3}[O_3(g)]} \tag{4}$$

Table 1 compares the fitting parameters for Figures 4 and 5 using eqs 2 and 4, respectively.

Product yield experiments were also performed at ozone concentrations of 8.2×10^{13} and 1.5×10^{15} molecules cm^{-3} at 48% and 57% RH, respectively. The presence of gas-phase water had no effect on the anthraquinone product yields at both ozone concentrations investigated within experimental error (see Figure 5). Possible explanations for this observation are presented in the Discussion.

4. Discussion

4.1. Reaction Kinetics under Dry and High Relative Humidity Conditions. To summarize our findings, the reaction between surface-bound anthracene and gas-phase ozone followed first-order kinetics with respect to anthracene loss under both dry and high relative humidity conditions. The dependence of k^I_{obs} on $[O_3(g)]$ was consistent with a reaction proceeding via a Langmuir−Hinshelwood mechanism, where one species is strongly adsorbed to the surface and a second gas-phase species is in equilibrium between the gas phase and the surface. The actual reaction is a two-step process: the adsorption of the gas-phase species (i.e., ozone) followed by the surface reaction. This is in contrast to a reaction that proceeds via an Eley−Rideal[29] reaction mechanism, which would display a linear dependence between the k^I_{obs} and $[O_3(g)]$. There was no change

TABLE 2: Comparison of Fitting Parameters for the Reaction of Surface-Adsorbed Anthracene and Surface-Adsorbed Benzo[*a*]pyrene with Ozone on Different Substrates

		substrate	$10^3 k^{I}_{max}$ (s^{-1})	$10^{15} K_{O_3}$ (cm^3)
anthracene	this work	Pyrex glass	6.4 ± 1.8	2.8 ± 0.9
	Mmereki et al.[13,14]	water	2.55 ± 0.17	0.466 ± 0.059
		stearic acid film on water	2.26 ± 0.20	0.520 ± 0.13
		1-octanol	2.59 ± 0.14	1.96 ± 0.34
		octanoic acid	1.11 ± 0.12	1.46 ± 0.62
		hexanoic acid	0.48 ± 0.07	0.847 ± 0.256
benzo[*a*]pyrene	Kwamena et al.[a]	azelaic acid aerosols (dry)[12]	48 ± 8	1.20 ± 0.04
		NaCl aerosol[12]	32[b]	<0.12
		soot aerosols[8]	15 ± 1	280.0 ± 20
		fused silica[9]	32[b]	28
		nonactivated silica[7]	32[b]	9.5

[a] Adapted from Kwamena et al.[12] [b] The value for k^{I}_{max} was assumed to be 0.032 s^{-1}, which is the average k^{I}_{max} of the results from Kwamena et al.[12] and Poschl et al.[8]

in the kinetics when the experiments were performed at higher relative humidities.

We compare our work with studies by Mmereki and co-workers[13,14] who have investigated the reaction of surface-adsorbed anthracene and ozone on different coated aqueous surfaces and also observed Langmuir−Hinshelwood behavior. The functional similarity between their results on aqueous surfaces and our results on a solid surface provides further evidence that the Langmuir−Hinshelwood reaction of surface-adsorbed anthracene and gas-phase ozone is a general mechanism in reactions of this type. Mmereki and co-workers[13,14] quote *A* and *B* parameters in their work, where the A parameter is the same as the k^{I}_{max} quoted here and the *B* parameter is the ratio of surface desorption to adsorption. However, when there is no ozone dissolution, as in the case of their air−aqueous interface experiments, the *B* parameter approximates to the inverse of K_{O_3}.[30] Therefore, the *B* parameters obtained by Mmereki et al.[13,14] were converted to K_{O_3} and the fitting parameters (K_{O_3} and k^{I}_{max}) for the different coated aqueous surfaces are summarized along with our results in Table 2.

The k^{I}_{max} from our work on Pyrex is within a factor of 3 of the work done by Mmereki et al.[13] on aqueous and stearic-acid and 1-octanol coated surfaces. This parameter is reduced even further when the reaction is performed in the presence of small acids (i.e., octanoic and hexanoic acids).[13,14] The similarity of the results on Pyrex, water, stearic acid and 1-octanol suggests that once the ozone is on the surface, the reaction proceeds at essentially the same rate, independent of any substrate effect. In contrast, the partitioning of O_3 to the surface demonstrates a stronger substrate effect. The K_{O_3} values, which describe the partitioning of ozone to the different substrates, vary over almost 3 orders of magnitude, when other values from the literature are included (see Table 2) in the comparison. It is curious to note that the K_{O_3} for our work on Pyrex is similar to the K_{O_3} obtained by Mmereki et al.[13] on the 1-octanol coated surface. One would not expect ozone to partition to Pyrex and 1-octanol, although they are both slightly polar, in a similar manner. We believe the presence of an organic contaminant with properties similar to 1-octanol may explain this observation. However, because it is most likely that anthracene is present as clumps or islands on the Pyrex tubes, we cannot rule out the possibility that ozone may be partitioning directly onto anthracene. In addition, as the reaction proceeds and the length of time for ozone exposure is increased, there is a buildup of anthraquinone on the surface. The presence of this more oxidized species may change the nature of the surface by making it more hydrophilic. As such, the K_{O_3} that we estimate may describe the partitioning of ozone to Pyrex, anthracene and/or the products of this oxidation reaction such as anthraquinone.

In our work investigating the reaction of surface-bound BaP on azelaic acid aerosols with ozone,[12] we also found that the primary factor driving the kinetics of the surface-bound reaction with ozone was the partitioning of ozone to the surface as described by K_{O_3}. Comparing the experimental and calculated literature k^{I}_{max} for the different substrates in our previous work found that they fell within a factor of 3 of each other; however, K_{O_3} varied over 3 orders of magnitude (see Table 2). These results imply that the aerosol surface is the main factor in determining the lifetime of the surface-bound PAHs because the nature of the surface determines the availability of the adsorbed ozone.

The experiments that were performed at higher relative humidities were done to test the effect of water vapor on the kinetics. To our knowledge, there have been no previous studies investigating the kinetics of surface-bound anthracene and ozone at elevated relative humidities. We found that the kinetics were unchanged under high relative humidity conditions. In our study[12] investigating the reaction of surface-bound BaP on azelaic acid aerosols with ozone at elevated RH, we found that the reaction kinetics were enhanced. In contrast, Poschl et al.[8] found that the reaction kinetics of surface-bound BaP on soot aerosols with ozone was reduced at higher RH.

For our azelaic acid substrate, we concluded that the partitioning of gas-phase water to the particle provided a substrate to which ozone had a greater affinity and therefore increased partitioning. Studies have shown that water adsorbs to oxidized organics, such as azelaic acid, in monolayer quantities at RH similar to those used in our experiments.[31,32] On the other hand, Pyrex may be too hydrophobic for water adsorption and, as a result, water may not have partitioned to the surface during our elevated RH experiments and thus the Pyrex surface remained unchanged.

Although the focus of past kinetic studies of this type has been on using the K_{O_3} to explain the partitioning of ozone to different substrates to account for the variability in the observed kinetics, these studies can also provide information about whether these surface reactions proceed in a diffusion-controlled manner or not. A study by Remorov and Bardwell[33] modeled the recombination of OH on the surface of nonreactive salts using the Langmuir−Hinshelwood reaction mechanism. They suggest that the diffusion-limited rate constant (k^{d}) is equal to approximately 10^{-5} cm^2 s^{-1}. Though this model was used to describe the reaction of two radical species, we assume that k^{d} can also be applied as an upper limit for our heterogeneous reaction.

The experimental second-order surface rate coefficient (k^{II}) obtained from this work for the reaction between surface-adsorbed anthracene and ozone falls within the range 10^{-13}−

10^{-16} cm^2 s^{-1}. We arrive at this range on the basis of the experimental values determined using eq 2 and assuming that the number of surface sites for ozone is between 10^{10} and 10^{14} molecules cm^{-2}. An upper limit for this reaction (k^{upper}) can also be estimated using the known rate constants for the corresponding gas-phase reaction and the layer thickness.[33] Therefore, if we assume that the rate constant for the gas-phase reaction of anthracene and ozone is within the range of the known rate constants for the gas-phase reaction of other PAHs and ozone, approximately $10^{-16}-10^{-19}$ cm^3 molecule^{-1} s^{-1},[1] and estimate our layer to be approximately one molecule thick, we obtain an upper limit for the reaction of $10^{-7}-10^{-10}$ cm^2 s^{-1}. Given that both k^{II} and k^{upper} are less than k^d we suggest that this reaction is not diffusion-limited and that the observed rates are due to a barrier in the reaction occurring between the molecules that lowers the rate to which molecules see each other via diffusion. These same conclusions may also be applied to the reaction of surface-bound BaP and ozone, which we studied previously.[12]

4.2. Product Identification and Yields: Implications for a Reaction Mechanism. In this study, we provide the first quantitative examination of one of the products of the reaction of surface-adsorbed anthracene and ozone: 9,10-anthraquinone. Anthraquinone product yields were obtained over an ozone concentration up to 9.1×10^{15} molecules cm^{-3} under dry conditions. The product yields displayed a nonlinear dependence on gas-phase ozone concentration (Figure 5). Modeling the data in Figure 5 using eq 3 and using eq 4 to interpret the results, we determine K_{O_3} and ANQ_{max}%: $K_{O_3} = (3.4 \pm 1.5) \times 10^{15}$ cm^3 and ANQ_{max} % $= 30 \pm 18$%. Experiments were also performed under high relative humidity conditions (RH $\sim$ 50, 60%) to determine if other product formation pathways may become more or less important and thus affect the anthraquinone yield. The product yields obtained at higher relative humidities were in good agreement with the anthraquinone yields that were observed under dry conditions (see Figure 5). The similarity in the product yields provides evidence that the same reaction mechanism may be responsible for anthraquinone formation under dry and high relative humidity conditions.

The K_{O_3} obtained from the product study under dry conditions was, within experimental error, in agreement with the K_{O_3} obtained from the kinetic study (Table 1). The shapes of Figures 4 and 5 demonstrate that both anthracene loss due to ozone and anthraquinone formation have the same dependence on ozone concentration: a dependence with Langmuir adsorption characteristics. Figure 5 also provides further evidence that the reaction of surface-bound anthracene and gas-phase ozone does proceed by the Langmuir−Hinshelwood reaction mechanism. This implies that the partitioning of ozone to the surface is an important step, i.e., the rate-limiting step, in the kinetics of anthracene loss and anthraquinone product formation. However, this does not imply that the rate-limiting step is the same step for these two processes. Although anthracene may react with adsorbed ozone, several reaction steps may occur to produce an intermediate that then reacts with ozone to form anthraquinone. The reaction between this intermediate and ozone will be the rate-limiting step in anthraquinone product formation. To our knowledge, this is the first piece of evidence that suggests ozone is directly involved in the rate-limiting step for the formation of anthraquinone.

This study also provides insight into the mechanism that governs the reaction. Bailey et al.[34] studied the reaction between anthracene and dissolved ozone in different solvent systems. The products observed included anthraquinone and phthalic acid.

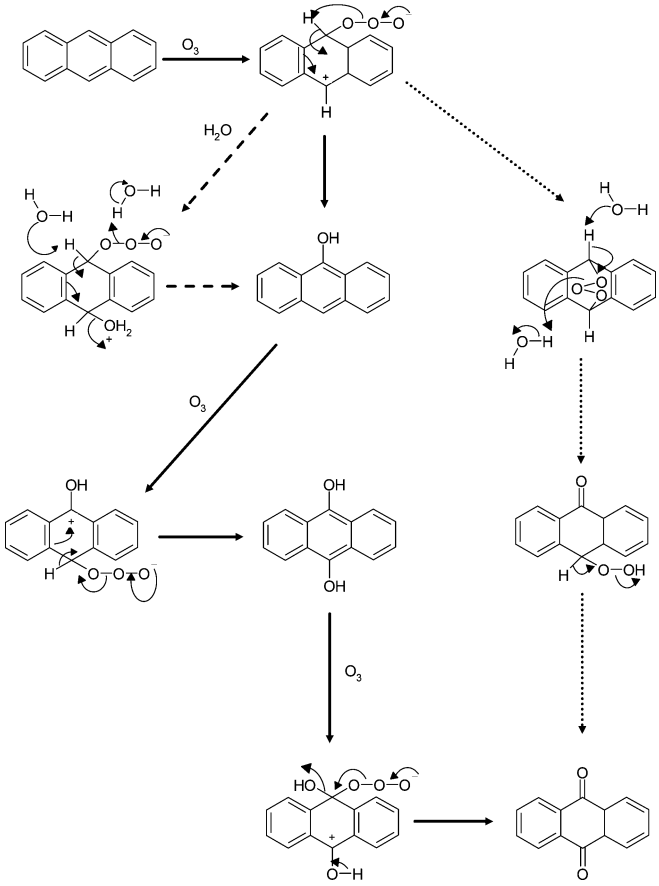

Figure 6. Reaction mechanism for the ozonation of anthracene to yield anthraquinone (adapted from Bailey et al.[34]). The mechanism outlined by bold arrows was proposed by Bailey and co-workers for the direct formation of anthraquinone and is suggested here to govern the heterogeneous reaction of surface-bound anthracene and ozone.

The reaction mechanism outlined in Figure 6 was proposed by Bailey et al.[16,34] to explain the anthraquinone formation in these different solvent systems. They also suggested that anthraquinone may be formed directly by ozonolysis and indirectly by the reduction of peroxide precursors in the workup steps. The anthraquinone yield by both direct and indirect formation combined was $\sim$70%. However, the yield for anthraquinone formed directly by ozonolysis was about 30%. This yield is in very good agreement with the maximum anthraquinone yield obtained in this study. The similarity in the yields may suggest that a similar reaction mechanism is at work even though the chemical environments in which they proceed are very different. The reaction mechanism outlined by the solid arrows in Figure 6 is the one proposed by Bailey et al.[34] for the direct formation of anthraquinone. Assuming that the reaction mechanism suggested by Bailey and co-workers applies to this study, three ozone molecules are required for anthraquinone formation. However, what cannot be determined on the basis of the results of this study is which reaction step with ozone is the rate-determining step and therefore results in the nonlinear dependence of the anthraquinone yield on ozone concentration.

Mmereki et al.[14] is the only other study that has investigated the products of the heterogeneous reaction between anthracene and ozone. Their experiments were performed using a Langmuir trough. Anthracene was adsorbed on a stearic acid−aqueous surface and on dry Teflon. The samples were exposed to high levels of ozone, approximately 10^{16} molecules cm^{-3}. Following extraction the samples were analyzed using GC−MS and anthracene loss was observed on both the stearic acid film and on dry Teflon. 9,10-Anthraquinone was observed as a product

on the surface and in the aqueous extract for the experiments on dry Teflon and the stearic acid film, respectively. Less anthracene was lost on the dry Teflon surface, but the amounts were not quantified. The reduced anthracene loss on the dry Teflon and the greater anthracene loss on the coated aqueous surface was hypothesized by Mmereki and co-workers to suggest that water may play a role in the mechanism.

The hypothesis proposed by Mmereki et al.[14] is in contrast to our observed results, which suggest that water vapor does not play a role in the anthraquinone formation pathway. In our experiments, to test the influence of water on the mechanism, we increased the concentration of the gas-phase water by increasing the RH, whereas in the studies by Mmereki et al.,[14] the water was already present on the surface. It is possible that in our study the water did not partition to the Pyrex/anthracene surface and therefore the water did not participate in the surface reaction. The Pyrex/anthracene surface may be too hydrophobic for the water to partition onto. However, with Mmereki et al.'s experimental approach the partitioning step was eliminated. If Pyrex is assumed to be a surrogate for an inert, hydrophobic aerosol substrate, high RH conditions may not influence the anthraquinone product yield, on the basis of the results of our study.

5. Atmospheric Implications and Conclusions

In this work we have shown that the reaction of anthracene adsorbed on Pyrex tubes and gas-phase ozone proceeds by the Langmuir−Hinshelwood mechanism. This result is in agreement with work by Mmereki et al.,[13] who were the first to investigate the kinetics of surface adsorbed anthracene and ozone and Poschl et al.,[8] who were the first to apply this reaction mechanism to the reaction of surface-adsorbed PAHs and ozone. We also performed a product study that profiled the anthraquinone product yield as a function of ozone concentration and RH. We observed a nonlinear dependence, similar to the Langmuir absorption plot, of the product yield on ozone concentration with a maximum yield of 30 ± 18%. To our knowledge, our study provides the first piece of direct evidence that ozone is directly involved in the rate-limiting step for anthraquinone formation. Experiments performed at increased RH did not influence the anthraquinone yields or the kinetics. Therefore, on the basis of our study at atmospherically relevant conditions ($[O_3](g) = 100$ ppb), the anthraquinone product yield would be very small, less than 1%, under both dry and high RH conditions. This implies that the oxidation of surface-bound anthracene, by ozone, may not be the dominant pathway for anthraquinone formation in the atmosphere. Given that anthraquinone is detected in the atmosphere,[17−19] we suggest that other reactions and direct emission may be responsible for its observed presence in the atmosphere.

Future work investigating the effect of ozone concentration on the other products of the reaction of surface-bound anthracene and ozone could provide further insight about its mechanism. These other products may include pthtalic acid, an endoperoxide, a quinone dimer and dihydroxyanthraquinone on the basis of previous studies in different chemical environments.[34−37] Recently, Kahan et al.[38] investigated the reaction of several PAHs (anthracene, pyrene, phenanthrene, naphthalene, and benzo[*a*]-pyrene) dissolved in a thin film of 1-octanol or decanol with ozone. They observed Langmuir−Hinshelwood behavior for all PAHs investigated. Based on this and other recent studies,[8,12−14] it seems reasonable to suggest that the reaction of surface-bound PAHs and ozone does proceed by the Langmuir−Hinshelwood mechanism and that the substrate dominates in determining their lifetimes with respect to ozone loss by influencing the degree of ozone partitioning to the surface. Further investigations with different oxidants, such as OH, NO_3, and HNO_3, should be performed to determine if these heterogeneous reactions of PAHs also proceed by the Langmuir−Hinshelwood mechanism and/or display a strong substrate effect.

Acknowledgment. We thank Dan Mathers of the ANALEST facility for use of the HPLC. Acknowledgment is made to the donors of the Petroleum Research Fund, administered by the American Chemical Society, for support of this work, as well as to NSERC. N.-O.A. K. thanks NSERC for the award of a PGS D Scholarship. We are also grateful to Jamie Donaldson for helpful comments regarding this manuscript.

References and Notes

(1) Finlayson-Pitts, B. J.; Pitts, J. N., Jr. *Chemistry of the Upper and Lower Atmosphere*; Academic Press: Toronto, 2000.
(2) Pierce, R. C.; Katz, M. *Environ. Sci. Technol.* **1975**, *9*, 347−353.
(3) Schwartz, J.; Laden, F.; Zanobetti, A. *Environ. Health Persp.* **2002**, *110*, 1025−1029.
(4) Pope, C. A., III; Burnett, R. T.; Thun, M. J.; Calle, E. E.; Krewski, D.; Ito, K.; Thurston, G. D. *J. Am. Med. Assoc.* **2002**, *287*, 1132−1141.
(5) Mar, T. F.; Norris, G. A.; Koenig, J. Q.; Larson, T. V. *Environ. Health Perspect.* **2000**, *108*, 347−353.
(6) Kotzick, R.; Panne, U.; Niessner, R. *J. Aerosol Sci.* **1997**, *28*, 725−735.
(7) Alebic-Juretic, A.; Cvitas, T.; Klasinc, L. *Environ. Sci. Technol.* **1990**, *24*, 62−66.
(8) Poschl, U.; Letzel, T.; Schauer, C.; Niessner, R. *J. Phys. Chem. A* **2001**, *105*, 4029−4041.
(9) Wu, C.-H.; Salmeen, I.; Niki, H. *Environ. Sci. Technol.* **1984**, *18*, 603−607.
(10) Kamens, R. M.; Guo, Z.; Fulcher, J. N.; Bell, D. A. *Environ. Sci. Technol.* **1988**, *22*, 103−108.
(11) Korfmacher, W. A.; Wehry, E. L.; Mamantov, G.; Natusch, D. F. S. *Environ. Sci. Technol.* **1980**, *14*, 1094−1099.
(12) Kwamena, N.-O. A.; Thornton, J. A.; Abbatt, J. P. D. *J. Phys. Chem. A* **2004**, *108*, 11626−11634.
(13) Mmereki, B. T.; Donaldson, D. J. *J. Phys. Chem. A* **2003**, *107*, 11038−11042.
(14) Mmereki, B. T.; Donaldson, D. J.; Gilman, J. B.; Eliason, T. L.; Vaida, V. *Atmos. Environ.* **2004**, *38*, 6091−6103.
(15) Van Cauwenberghe, K. Atmospheric Reactions of PAHs. In *Handbook of Polycyclic Aromatic Hydrocarbons: Emission Sources and Recent Progress in Analytical Chemistry*; Bjorseth, A., Ramdahl, T., Eds.; Marcel Dekker Inc: New York, 1985; Vol. 2, pp 351−385.
(16) Bailey, P. S.; Sinha, B.; Kolsaker, P.; Dobinson, F.; Ashton, J. B.; Batterbee, J. E. *J. Org. Chem.* **1964**, *29*, 1400−1409.
(17) Konig, J.; Balfanz, E.; Funcke, W.; Romanowski, T. *Anal. Chem.* **1983**, *55*, 599−603.
(18) Pierce, R. C.; Katz, M. *Environ. Sci. Technol.* **1976**, *10*, 45−51.
(19) Ligocki, M. P.; Pankow, J. F. *Environ. Sci. Technol.* **1989**, *23*, 75−83.
(20) Choudhury, D. R. *Environ. Sci. Technol.* **1982**, *16*, 102−106.
(21) Ramdahl, T. *Environ. Sci. Technol.* **1983**, *17*, 666−670.
(22) Pitts, J. N., Jr.; Lokensgard, D. M.; Ripley, P. S.; van Cauwenberghe, K. A.; Van Vaeck, L.; Shaffer, S. D.; Thill, A. J.; Belser, W. L. *Science* **1980**, *210*, 1347−1349.
(23) Fatiadi, A. J. *Environ. Sci. Technol.* **1967**, *1*, 570−572.
(24) Pitts Jr, J. N.; van Cauwenberghe, K. A.; Grosjean, D.; Schmidt, J. P.; Fritz, D. R.; Belser Jr, W. L.; Knudson, G. B.; Hynds, P. M. *Science* **1978**, *202*, 515−519.
(25) Kamens, R.; Bell, D.; Dietrich, A.; Perry, J.; Goodman, R.; Claxton, L.; Tejada, S. *Environ. Sci. Technol.* **1985**, *19*, 63−69.
(26) Pedersen, D. U.; Durant, J. L.; Penman, B. W.; Crespi, C. L.; Hemond, H. F.; Lafleur, A. L.; Cass, G. R. *Environ. Sci. Technol.* **2004**, *38*, 682−689.
(27) Kamens, R. M.; Karam, H.; Guo, J.; Perry, J. M.; Stockburger, L. *Environ. Sci. Technol.* **1989**, *23*, 801−806.
(28) *Spectral Atlas of Polycyclic Aromatic Compounds*; Kluwer Academic Publishers: Boston, 1998; Vol. 2.
(29) Adamson, A. W. *Physical Chemistry of Surfaces*, 5th ed.; John Wiley and Sons: Toronto, 1990.
(30) Donaldson, D. J. *J. Phys. Chem. A.* **1999**, *103*, 62−70.
(31) Demou, E.; Visram, H.; Donaldson, D. J.; Makar, P. A. *Atmos. Environ.* **2003**, *37*, 3529−3537.

(32) Thomas, E.; Rudich, Y.; Trakhtenberg, S.; Ussyshkin, R. *J. Geophys. Res.* **1999**, *104*, 16053−16059.

(33) Remorov, R. G.; Bardwell, M. W. *J. Phys. Chem. B* **2005**, *109*, 20036−20043.

(34) Bailey, P. S. In *Ozonation in Organic Chemistry*; Academic Press: Toronto, 1982.

(35) Fox, M. A.; Olive, S. *Science* **1979**, *205*, 582−583.

(36) Grosjean, D.; Whitmore, P. M.; De Moor, C. P.; Cass, G. R.; Druzik, J. R. *Environ. Sci. Technol.* **1987**, *21*, 635−643.

(37) Dabestani, R.; Ellis, K. J.; Sigman, M. E. *J. Photochem. Photobiol. A-Chem.* **1995**, *86*, 231−239.

(38) Kahan, T. F.; Kwamena, N. O. A.; Donaldson, D. J. *Atmos. Environ.*, accepted for publication.